Dressing protective clothing: stabilizing alizarin/halloysite hybrid pigment and beyond

Guanzheng Zhuang, Francisco Rodrigues, Zepeng Zhang, Maria Gardennia Fonseca, Philippe Walter, Maguy Jaber

Dressing protective clothing: stabilizing alizarin/halloysite hybrid pigment and beyond

Guanzheng Zhuang [a, b], Francisco Rodrigues [a,c], Maria Gardennia Fonseca[d], Zepeng Zhang [b, *], Philippe Walter [a], and Maguy Jaber [a, *]

[a] Sorbonne Université, Laboratoire d'Archéologie Moléculaire et Structurale (LAMS), CNRS UMR 8220, case courrier 225, UPMC 4 Pl. Jussieu, 75005 PARIS CEDEX 05, France.

[b] Beijing Key Laboratory of Materials Utilization of Nonmetallic Minerals and Solid Wastes, National Laboratory of Mineral Materials, School of Materials Science and Technology, China University of Geosciences, Xueyuan Road, Haidian District, Beijing 100083, PR China.

[c] Chemistry Department of Universidade Estadual da Paraíba, Campina Grande, Paraíba, Brazil

[d] Universidade Federal da Paraíba, Cidade Universitária, - Laboratório de Combustíveis e Materiais (NPE –LACOM). s/n - Castelo Branco III, 58051-085, João Pessoa - PB, Brazil.

Corresponding Author:

Maguy Jaber

Email: maguy.jaber@upmc.fr

Zepeng Zhang

Email: unite508@163.com

Abstract

The fading of organic dyes is a serious challenge for conservation of art works. Inspired by the ancient Maya blue pigment, a hybrid pigment of halloysite (Hal) and alizarin (AZ) was prepared by adsorption in aqueous solution. In addition, a layer of polyorganosilane (POS) is used to cover the surface of the hybrid pigment to enhance the chemical resistance and photostability. The hybrid pigments were characterized by X-ray diffraction, transmission electron microscopy, Fourier transform infrared and thermal analysis. The adsorption behavior of AZ onto Hal was investigated and optimized. AZ-Hal hybrid pigment was prepared at pH = 9. Chemical stability was checked by 1 mol/L HCl, 1 mol/L NaOH and ethanol attack. Photostability was evaluated by exposing the pigment to visible light for 360 h, which is equal to more than 28 years in a common museum. AZ molecules were adsorbed on the external and/or internal surface via physical adsorption and hydrogen bonds. The presence of POS in the hybrid pigment influences positively the chemical and light resistance. This may be due to the protective layer that isolates sensitive dyes and oxidizing agents.

Keywords: hybrid pigments, clay minerals, adsorption, organosilane, stability

1. Introduction

Organic dyes and pigments commonly used in traditional painting was limited to selected natural materials available [1] before the boom of the modern chemical industry in the 19th century. In traditional fine art, namely in easel painting, polychrome art, manuscript illumination, textile and other historic works of art, the derivatives of anthraquinone (alizarin, carmine, laccaic acids, and related red dyes) were widely used in the form of lakes. The colorants reflect important artistic and historical values and may provide clues to the understanding of ancient cultures. The use of organic dyes is usually challenged by fading, due to light exposure [2, 3], thermal and chemical attack, as well as the color change in pH [3, 4]. The poor stability of organic dyes can dramatically affect the appreciation of a work of art and induces the deterioration of the later.

Anthraquinones are classified as the natural organic dyes most resistant to light induced deterioration used since prehistoric times [5, 6]. These colorants are extracted from the roots of *Rubia tinctorum* L., which is the source of madder. The madder belongs to one of the most important groups of red dyestuffs of the family of Rubiaceae. Alizarin (1,2-dihydroxyanthraquinone, abbreviated as AZ, see Fig. 1) is one of the principal occurring dyes in *Rubia tinctorum* L. [5, 7]. It is the most

important constituent of the madder lake dye [8], which is a pigment precipitated on an inert inorganic substrate ($Al_2O_3 \cdot H_2O$) [9]. AZ has been extensively employed in Asia since ancient times for dyeing textile materials. Madder was used as early as the sixteenth century BC in Egypt for dyeing. In the seventeenth and eighteenth centuries, AZ was increasingly used in paintings.

Enhancing the stability of colorants is of great interest for artists, archeologists and scientists. One possibility is to prepare organic-inorganic hybrids pigments where a strong interaction between organic chromophores and inorganic matrices aims to obtain stable pigments [10]. The famous example is the Maya blue pigment, an ancient hybrid pigment found in Mesoamerica. It was testified as a hybrid of palygorskite, a fibrous clay mineral, and natural indigo. Maya blue pigment shows excellent stability even after thousands of years. The color is not discharged by boiling nitric acid nor by heating much below redness [11]. Inspired by the ancient durable Maya blue pigment, a series of clay minerals were used to prepare clay/dye hybrid pigments, including montmorillonite [12-20], palygorskite [21-27], sepiolite [28-33] etc.

Halloysite (Hal) ($Al_2(OH)_4Si_2O_5 \cdot 2H_2O$) [34], a natural nanotubular clay mineral, is a promising host for organic-inorganic hybrid pigments. Generally, the length of halloysite nanotubes varies from ca. 0.02 to 30 μm and the external diameter from ca. 30 to 190 nm, with an internal diameter range of ca. 10-100 nm [35, 36]. The very large diameter of the halloysite tubes makes it potentially suitable for the accommodation of a range of guests. Zhang et al. [37] reported the preparation of

halloysite/$CoAl_2O_2$ hybrid pigment and its application in water-based paintings. Mico-Vicent et al. [38] prepared a hybrid pigment based on Hal and indigo carmine. The hybrid pigment showed worse thermal stability and a little better stability to pH. However, they didn't characterize the fading of pigment under light.

Hal can be a promising substrate for AZ, due to the large amount of hydroxyl groups and surface oxygen atoms, and the tubular morphology. Particularly, AZ is a pH-sensitive dye due to the phenolic hydroxyl groups. The solubility and color are pH dependent. To overcome this problem, a protective layer is considered to cover the surface. Previously, a protective layer of SiO_2 [22, 25] and polyorganosilane (POS) [21, 26] covering hybrid pigment surface were reported without going further in the study of photostability of the functionalized hybrid pigments.

Aiming to enhance the stability of AZ, a hybrid pigment of Hal and AZ was prepared by adsorption in aqueous solution. AZ-Hal hybrid pigment was covered with POS. The structures and resistance to acid, base, solvent and light were comparatively investigated.

2. Materials and Methods

2.1 Materials

Hal, AZ, n-hexadecyltrimethoxysilane (HDTMS, purity of 85%) and tetraethoxysilane (TEOS, purity of 99%) were purchased from Sigma-Aldrich, Inc, France. These materials were used without further purification. HCl (36.8%), NaOH (98.8%) and ethanol (95%) were purchased from VWR Co. Ltd. NaOH solution (1

mol/L) was prepared by dissolving NaOH solids into water. HCl solution (1 mol/L) was prepared by diluting the concentrated HCl.

2.2 Preparation of hybrid pigments

AZ-Hal pigment was obtained by adsorption process. 100 ppm of AZ solution was prepared at pH 9 after being treated with ultrasound for 10 min. 1 g of Hal was added into 100 mL of previous AZ solution and the adsorption was allowed to last for 4 h. After centrifugation, heating the resulting solid at 50°C for 24 h and grinding, AZ-Hal hybrid pigment was obtained. AZ-Hal-POS pigments were prepared by polycondensation of HDTMS and TEOS in the presence of Az-Hal pigment. 0.5 g of the AZ-Hal pigment was fully dispersed in 9 mL of ethanol and 1 mL of ammonia saturated in ethanol, magnetically stirred for 3 min in a vial. Then, TEOS and HDTMS (both concentration of 0.15 mol/L) were charged into the mixture with stirring. The dispersion was ultrasonicated for 30 min at 50° C, and then 1.44 mL of water was injected quickly into the dispersion under ultrasonication. The vial was sealed and ultrasonicated at 50° C for 1 h. The products were centrifuged at 6000 rpm for 5 min to remove the supernatant followed by washing 3 times each with ethanol. Then, the superhydrophobic AZ-Hal-POS pigment was obtained after drying at 50° C for 24 h.

2.3 Characterization

X-ray diffraction (XRD) test was conducted on a Bruker D8 diffractometer operating at Cu Kα radiation, 40 kV, 30 mA, and a scan speed of 0.77 s per step (step size of 0.04°) from 5° to 70°. Fourier transform infrared (FTIR) spectra were collected

from a Cary 630 FTIR spectroscopy in the range of 4000-650 cm^{-1}. Thermogravimetric (TG) analysis was carried out at a TA-SDTQ600 type analyzer from room temperature to 900°C under air, with the heating rate of 10°C/min. Transmission electron microscopy (TEM) was performed on a Tecnai Spirit G2 transmission electron microscope with the voltage of 120 kV. The samples were dispersed in ethanol with ultrasound for 30 min, then the dispersions were dropped on copper supports with carbon grid. The absorbance, reflectance and CIE (Commission Internationale de L'Eclairage) parameters were obtained from an Ocean Optics spectrometer USB4000. The light source of Ocean Optics DH-2000-BAL was used for absorbance, and HL2000 light source was employed for reflectance and CIE results. CIE 1976 color space system was applied to evaluate the color of the pigments. Lightness (L*) represents the brightness (+) or darkness (-) of the color, i.e., more positive L* values refer to whiter while more negative L* values represent darker. The values of a* and b* indicate the color details: +a* is the red direction, -a* the green direction, +b* the yellow direction, and -b* the blue direction. Before the reflectance and CIE tests, the samples were pressed into pellets with the pressure about 10 MPa. The total change in color was calculated as $\Delta E^* = \sqrt{(L_1^* - L_0^*)^2 + (a_1^* - a_0^*)^2 + (b_1^* - b_0^*)^2}$, where L_1* refers to the L* value of a sample, L_0* refers to the L* value of the reference, and similar to the other two parameters. Photostability was evaluated under visible lights for 360 h using an Advanced Illumination SL164 type LED light. The working distance between the light and the samples is 10 cm, corresponding to a diameter of 3.6 cm of working area,

with the minimum and typical irradiances of 138.6 and 163.0 W/m^2, minimum and typical illuminances of 46.7 and 54.9 kLux.

3. Results and discussion

3.1 Adsorption of alizarin onto Hal

AZ has two phenolic hydroxyl groups, which can release protons (Fig. 1). Two acid-basic equilibria happen when AZ is in aqueous solution. Kuban and Havel (1973) [39] reported the pK_{a1} = 5.25 and pK_{a2} = 11.50 of AZ. Later, Miliani et al. (2000) [9] reported the pK_{a1} and pK_{a2} values as 6.57 and 12.36, respectively. Hence, pH value directly influences the proportion of AZ, AZ^-, AZ^{2-} and H^+. Accordingly, the solubility of AZ in water and the color of AZ aqueous solution are sensitively affected by the pH value. In solid state, AZ is yellow powder. However, the color of AZ aqueous solution changes from yellow to red, and further to violet and blue with the increase of pH value. In addition, at low pH, AZ shows very poor solubility.

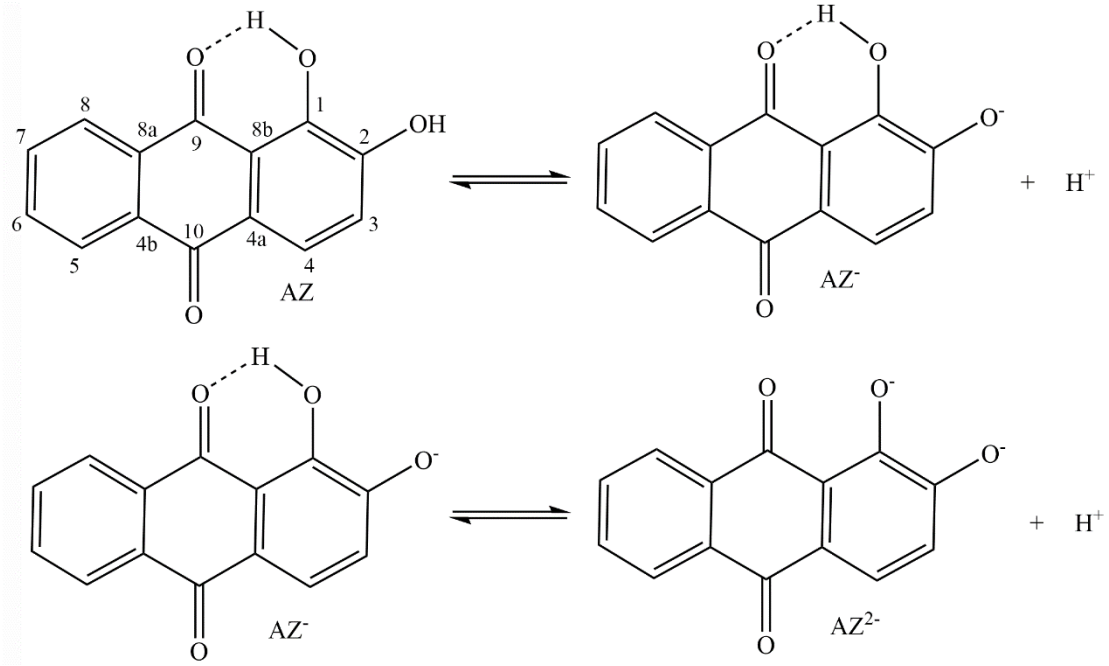

Fig. 1 Structure and acid-basic equilibria of AZ in aqueous solution.

To investigate the adsorption of AZ (97%) onto Hal, AZ aqueous solution with the concentration of 100 ppm and pH = 9 was used firstly. The adsorption capacity (q_e) at different time is presented in Fig. 2 (A). AZ was rapidly adsorbed onto Hal within 1 h and gradually got equilibrium at 4 h. Higher pH values promoted the solubility of AZ in aqueous solution, but higher pH values showed negative influence on the adsorption capacity (see Fig. 2 (B)). With the increase of pH value, the adsorption capacity decreased from 9.82 mg/g at pH = 9 to 4.81 mg/g at pH = 13. This can be correlated to the low negative charge of Hal. Recently, Pasbakhsh et al. (2013) [40] investigated the zeta potential of the six halloysites throughout the pH range and concluded that the halloysite had a significantly negative surface charge in the main pH range. As a result, halloysite tends to have a polyanionic surface, except at very low pH values. Hence, higher pH resulted in more AZ^- and AZ^{2-} anions, which led to the electrostatic repulsion with Hal surface.

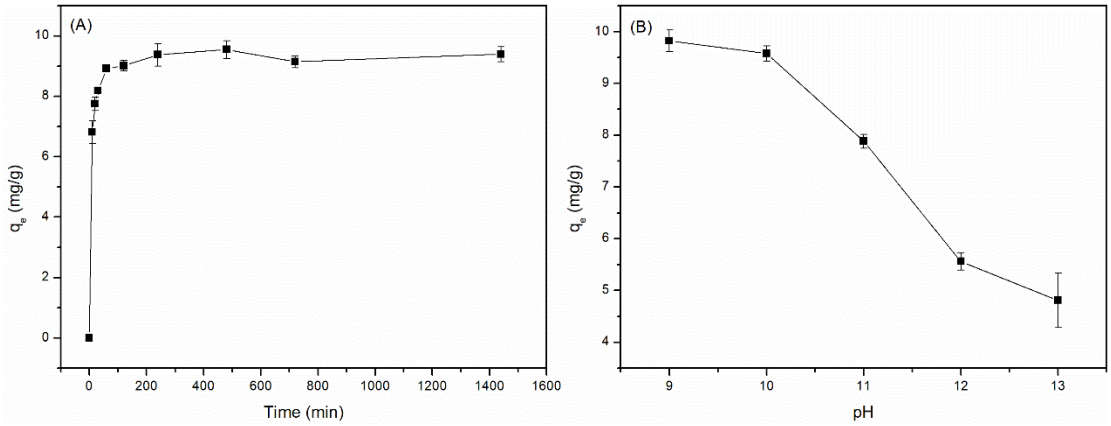

Fig. 2 Effect of (A) reaction time (c (AZ) = 100 ppm, pH = 9) and (B) pH (c (AZ) = 100 ppm, reaction time = 4 h) on the adsorption capacity of AZ onto Hal.

There is no doubt that the concentration of AZ has significant effect on the adsorption capacity. However, an important conflict should be pointed out. To improve the solubility of AZ in aqueous solution, it is necessary to increase the pH value. But high pH values result in the decline of the adsorption capacity. Hence, the adsorption capacities of AZ onto Hal with different mass ratios of AZ to Hal were studied (Fig. 3). The q_e increased with the increase of m_{AZ}/m_{Hal} from 4.69 mg/g with m_{AZ}/m_{Hal} = 5 mg/g to 38.55 mg/g with m_{AZ}/m_{Hal} = 100 mg/g. However, the adsorption efficiency of AZ decreased with the increase of m_{AZ}/m_{Hal} ratio, indicating more AZ molecules still remained in the solution. The digital pictures also support this phenomenon. Although the color of the hybrid pigments (Fig. 3 (C)) got darker with the increase of m_{AZ}/m_{Hal} ratio, the resulting solutions are also redder. Considering the influence of pH and m_{AZ}/m_{Hal} ratio on the solubility and adsorption capacity of AZ onto Hal, pH = 9 and m_{AZ}/m_{Hal} ratio of 20 mg/g are optimal. The adsorption capacity at these conditions is 16.60 mg/g.

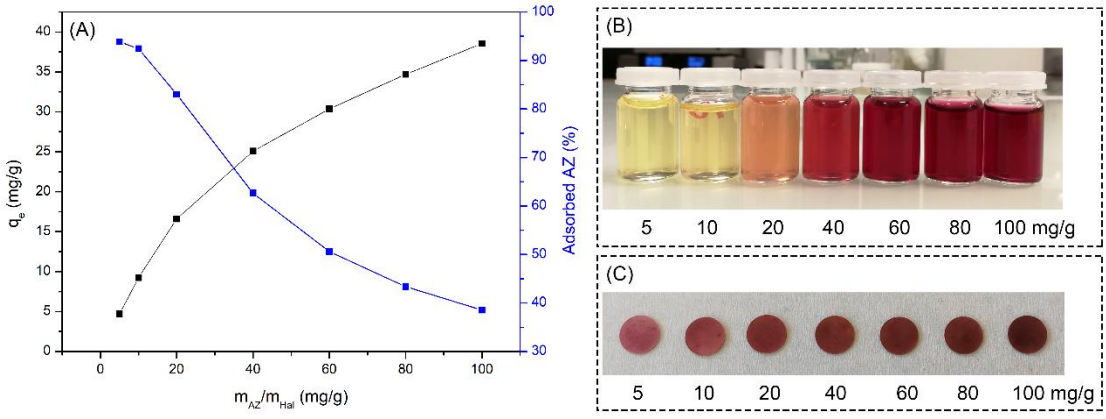

Fig. 3 (A) Adsorption capacity of AZ onto Hal at different ratios of m_{AZ}/m_{Hal} (concentration of 100 ppm), digital pictures of (B) resulting solutions and (C) the color of hybrid pigments.

3.2 Characterization of hybrid pigments

3.2.1 XRD

Typical reflections of halloysite are observed in the XRD pattern of Hal (Fig. 4), with the basal spacing of 0.75 nm. In addition, some reflections belonging to quartz and albite emerged. But the low intensity indicates the low content. AZ powder shows crystalline structure. After adsorption and covering by POS, the hybrid pigments showed the similar XRD patterns to the raw Hal. Especially, the hybrid pigment showed the same basal spacing of Hal, demonstrating that AZ molecules or derivatives didn't intercalate into the interlayer space. No reflections assigned to AZ were observed in the XRD patterns of hybrid pigments. This interesting phenomenon indicates that AZ molecules and its derivatives adsorbed on the surface of Hal by re-organizing arrangement of molecules.

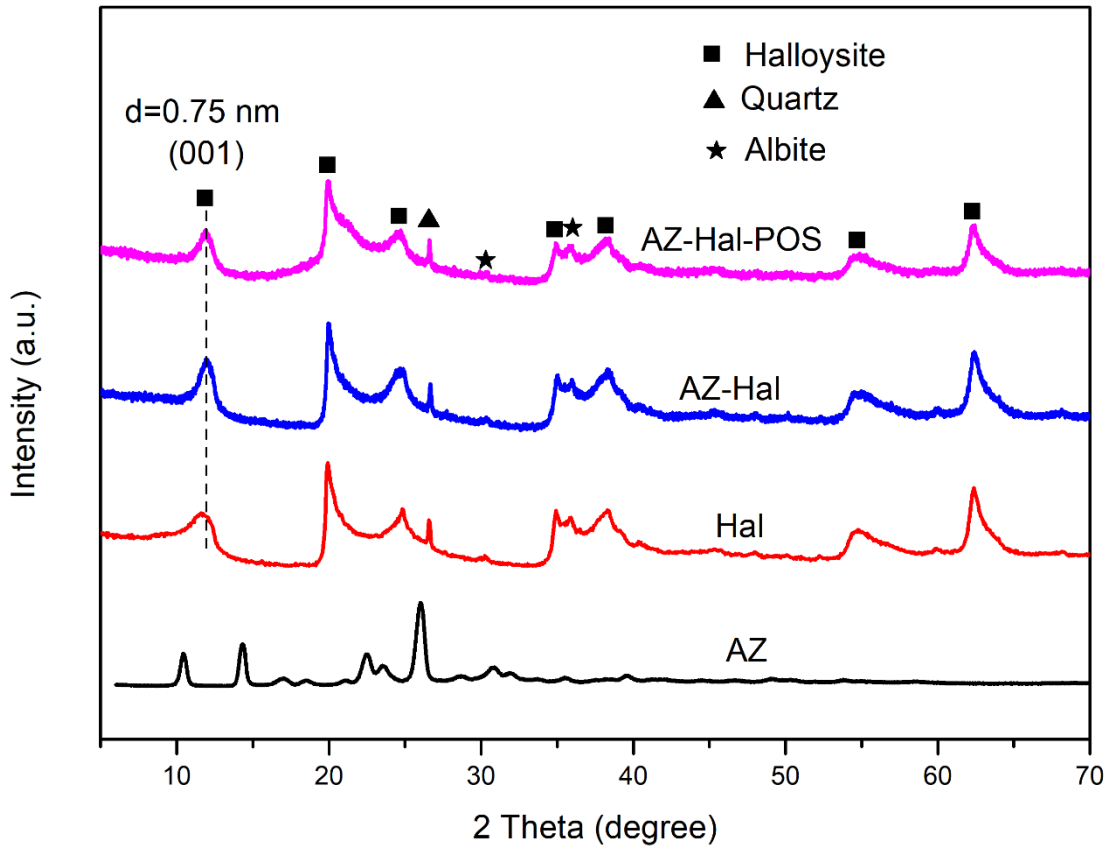

Fig. 4 XRD patterns of Hal, AZ and hybrid pigments.

3.2.2 TEM

The TEM images of Hal (Fig. 5 (A) and (B)) show the tubular morphology, with an inner diameter of 10-20 nm and an external diameter of 30-50 nm. The nanotubular morphology of Hal contributes to large surface area, which can accommodate many guest molecules. AZ-Hal presents the similar morphology with Hal, because the adsorption of AZ didn't affect the crystalline structure and morphology of Hal. Although AZ-Hal-POS shows the tubular morphology, the covering of POS changes the surface and arrangements of the nanotubes. Hal and AZ-Hal present clean surface while obvious organic surface is observed in SEM image of AZ-Hal-POS. POS mostly covered the nanotubes in groups, instead of single tube.

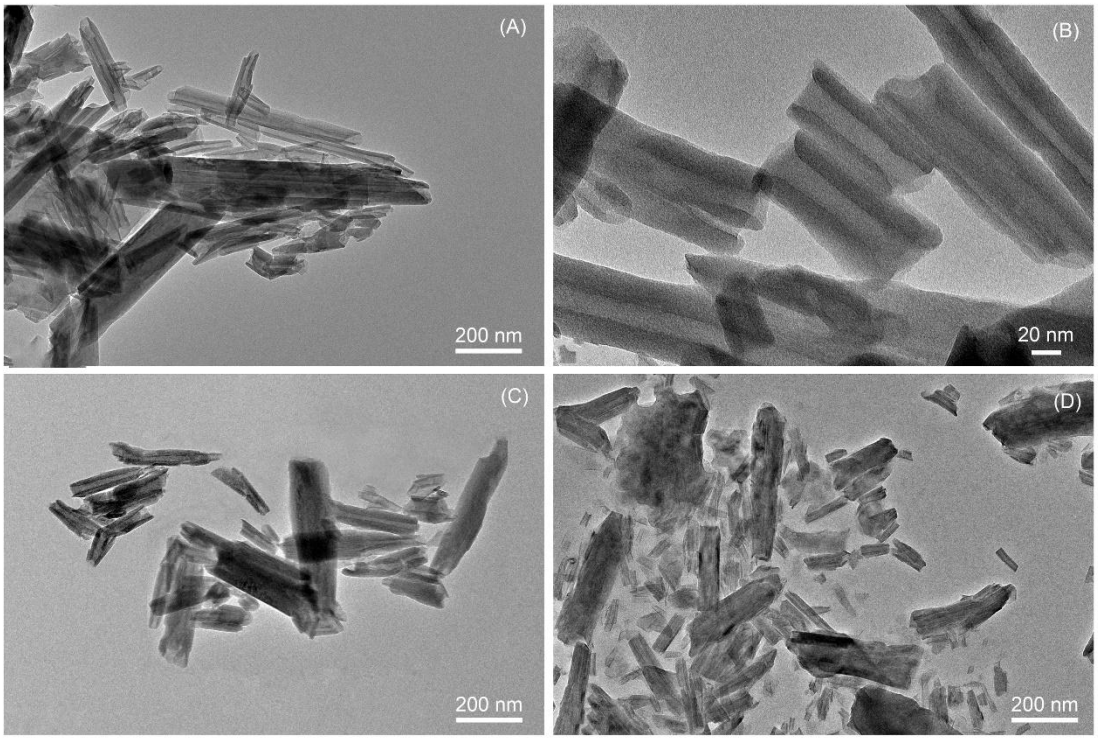

Fig. 5 TEM images of (A) and (B) Hal, (C) AZ-Hal and (D) AZ-Hal-POS.

3.2.3 FTIR

The FTIR spectrum of AZ is illustrated in Fig. 6 (A). According to the previous reports [10, 41-43], the assignments are summarized. The absorption band at 3372 cm^{-1} belongs to the vibration of phenolic hydroxyl groups of AZ. The characteristic bands of Alizarin are ν(10-C=O) at 1662 cm^{-1}; ν(9-C=O) at 1632; ν(Ar C=C) at 1586 and 1452 cm^{-1}; δ(OH) at 1349 and 1330 cm^{-1}; ν(C–O) at 1285 and 1266 cm^{-1} and carbonyl C–C–C at 1196 cm^{-1}. The bands of ν(9-C=O) at 1632 cm^{-1} and ν(10-C=O) at 1662 cm^{-1} appear separated because of the intramolecular hydrogen bonding between 9-C=O and 1-OH (see Fig. 1). The FTIR spectrum of Hal (Fig. 6 (B)) demonstrates the presence of inner-surface -OH (3693 cm^{-1}), inner -OH (3622 cm^{-1}) and surface adsorbed water (3548 cm^{-1}) [44-46]. The bands at 1652 cm^{-1} and 1632 cm^{-1}

correspond to the bending vibration H_2O and -OH groups, respectively. The band at 1118 cm^{-1} is attributed to the bending vibration of apical Si-O groups. The bending in-plane of Si-O-Si groups results in the two absorptions at 1002 cm^{-1} [45]. The bands observed at 906 cm^{-1} are caused by the O–H deformation of inner-surface hydroxyl groups, and O–H deformation of inner hydroxyl groups, respectively [47].

The absorption bands of Hal can be observed in the FTIR spectrum of AZ-Hal, except for some little shifts. Particularly, the vibration of structural -OH shifted from 1632 cm^{-1} to 1636 cm^{-1}. The most important changes appear in the range of 1700-1200 cm^{-1}, which indicate the interaction between AZ and Hal. Indeed, the bands of the two C=O groups and structural -OH were overlapped by the vibration of H_2O at 1653 cm^{-1}. The vibration of C=C (Ar) splits into 4 bands at 1592, 1530, 1469 and 1457 cm^{-1}. In AZ molecules, the benzene ring was conjugated with C=O groups. The split of benzene bands suggests some interaction between C=O groups and Hal surface, such as hydrogen bonds between C=O groups in AZ and -OH groups in Hal. δ(OH) increased from 1349 and 1330 cm^{-1} (AZ) to wide bands at 1354 cm^{-1} (AZ-Hal), demonstrating the chemical environment of -OH in AZ changed. The vibration of (C–O) at 1285 and 1266 cm^{-1} increased to 1290 and 1267 cm^{-1}, perhaps due to the interaction between -OH and Hal. In summary, AZ molecules were adsorbed on the Hal surface and interaction between the -OH and C=O groups of AZ and Hal surface happened. Hydrogen bonds are most likely to form between the C=O and HO-Al(Si) and/or between C-OH groups and O-Si(Al).

In the polycondensation process of organosilane, some adsorbed AZ dissolved

into the solution due to the basic NH_3. In the FTIR spectrum of AZ-Hal-POS (Fig. 6 (D)), the bands at 2921 and 2958 cm^{-1} belong to the $-CH_3$ and $-CH_2$ groups from organosilane. δ(C-H) occurred at 1466 and 1379 cm^{-1}. The absorption representing Si-O-Si (999 cm^{-1}) displays higher intensity than Hal and AZ-Hal, indicating crosslinking between organosilanes. These evidences testify that POS was successfully covered on the surface of hybrid pigment. Due to the low proportion of AZ, only weak signals are observed at 1358 cm^{-1} (C=O) and 1292 (C-O). These two bands occurs at the similar wavenumbers to C=O and C-O groups in AZ-Hal, implying covering with POS seldom affects the interaction between AZ and Hal.

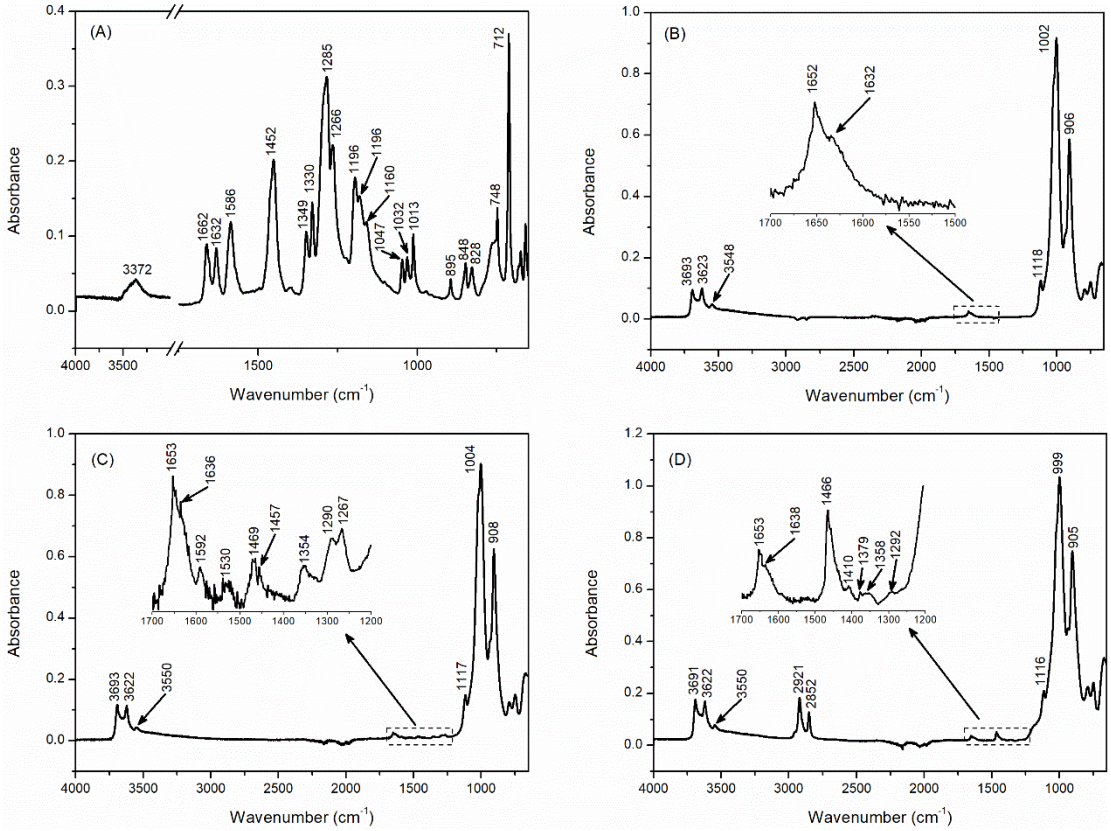

Fig. 6 FT-IR spectra of (A) AZ, (B) Hal, (C) AZ-Hal and (D) AZ-Hal-POS.

3.2.4 Thermal analysis

The TG and derivative TG (DTG) curves of materials and hybrid pigments are presented in Fig. 7. Four mass loss steps are observed in the TG/DTG curves, i.e., (i) the loss of adsorbed water at 58°C, (ii) loss of interlayer water at 154°C and (iii) dehydroxylation process in Al-OH and Si-OH groups at 485°C. The main oxidation of AZ occurs at 200-400°C, with the mass loss of 91.3%. Continuous oxidation stopped above 600°C. The TG/DTG curves of AZ-Hal are similar with Hal. A weak signal at 338°C is detected from the DTG curve. This mass loss process represents the oxidation of AZ in AZ-Hal hybrid pigment. Compared with the TG/DTG curves of AZ, AZ in AZ-Hal shows a little higher oxidation temperature, maybe because of the hydrogen bonding between AZ and Hal. 1.7% of adsorbed water is present in AZ-Hal-POS hybrid pigment. The mass loss between 250 and 400°C is attributed to the thermal decomposition of POS. The oxidation of AZ is overlapped. 14.3% of POS is estimated to cover the hybrid pigment.

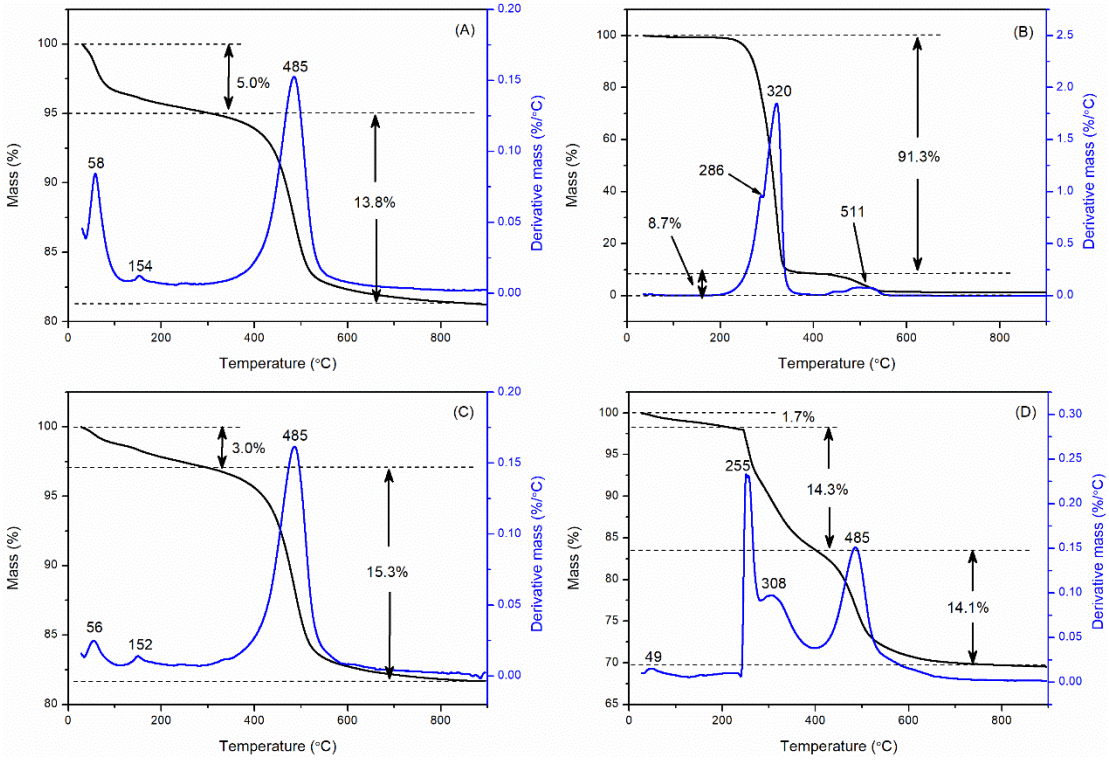

Fig. 7 TG and corresponding DTG curves of (A) Hal, (B) AZ, (C) AZ-Hal and (D) AZ-Hal-POS.

3.3 Color characterization and stability

AZ-Hal-POS present higher reflection than AZ-Hal in the visible light wavelength (Fig. 8). The dominant reflections occur at the wave length of more than 650 nm, implying the red color. Weak reflections in the range of 350-450 nm, which represent violet-blue color, are observed. The dissociation equilibrium of AZ depends on the pH value. AZ occurs in the form of partially dissociated yellow molecules at pH below 5.2. At pH 6–10 it is deprotonated and occurs in red monovalent cations. Finally, it occurs in the violet di-anionic form at pH about 12 [16]. The adsorption of AZ onto Hal took place at the pH value of 9. Due to the equilibria, AZ, AZ^-, AZ^{2-} and H^+ were included in the solution. A little AZ^{2-} can be also adsorbed onto Hal surface, resulting in the violet reflection. AZ-Hal-POS shows higher reflection between 350-450 nm, because the basic solution resulted from saturated ammonium/ethanol solution. The presence of ammonium in the process of covering with POS promote the dissociation of AZ molecules and produced more AZ^{2-}. The higher reflection of AZ-Hal-POS in the red range. The L*, a* and b* values (Table 1 and Table 2) precisely reveal the color of the hybrid pigments. A slightly higher L* value of AZ-Hal-POS than AZ-Hal demonstrates that AZ-Hal-POS is brighter than AZ-Hal. The positive a* values suggest red color and positive b* value indicate yellow. The a* and b* values demonstrate the mixed color of red and yellow, but red is dominant while yellow is

weak. AZ-Hal-POS exhibits more red and less yellow than AZ-Hal.

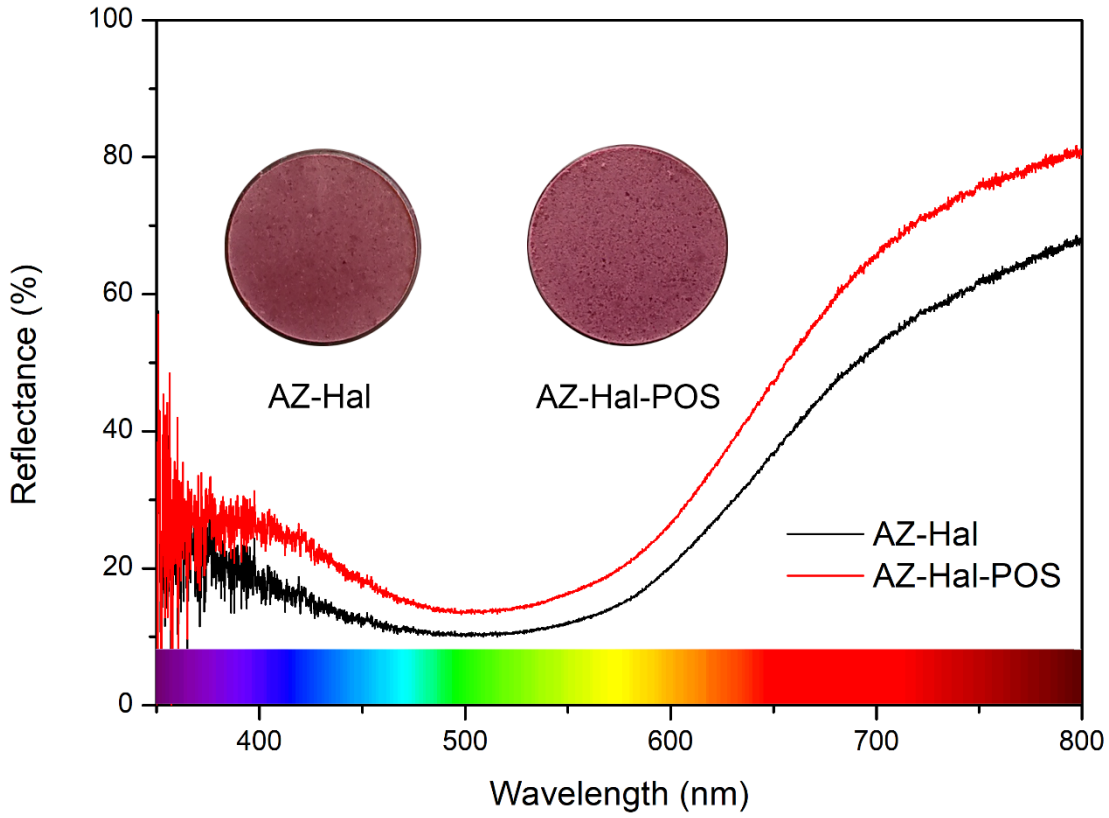

Fig. 8 Reflection spectra of AZ-Hal and AZ-Hal-POS.

The hybrid pigments were added into HCl (1 mol/L), NaOH (1 mol/L) and ethanol with the stirring for 24 h to check the chemical stability. The absorption results of the resulting solutions are applied to evaluate the dissolved dyes (Fig. 9). The resulting solution of HCl-treated pigments show a bit yellow color. The dominant absorptions emerge at less than 450 nm (violet-blue), indicating the complementary color of yellow. The HCl-treated solution of AZ-Hal exhibited much more adsorption than that of AZ-Hal-POS, demonstrating much more dyes dissolved into the solution. Similar

phenomena are observed in the NaOH- and ethanol-treated solutions. Treated by different chemicals, AZ-Hal-POS shows better stability than AZ-Hal.

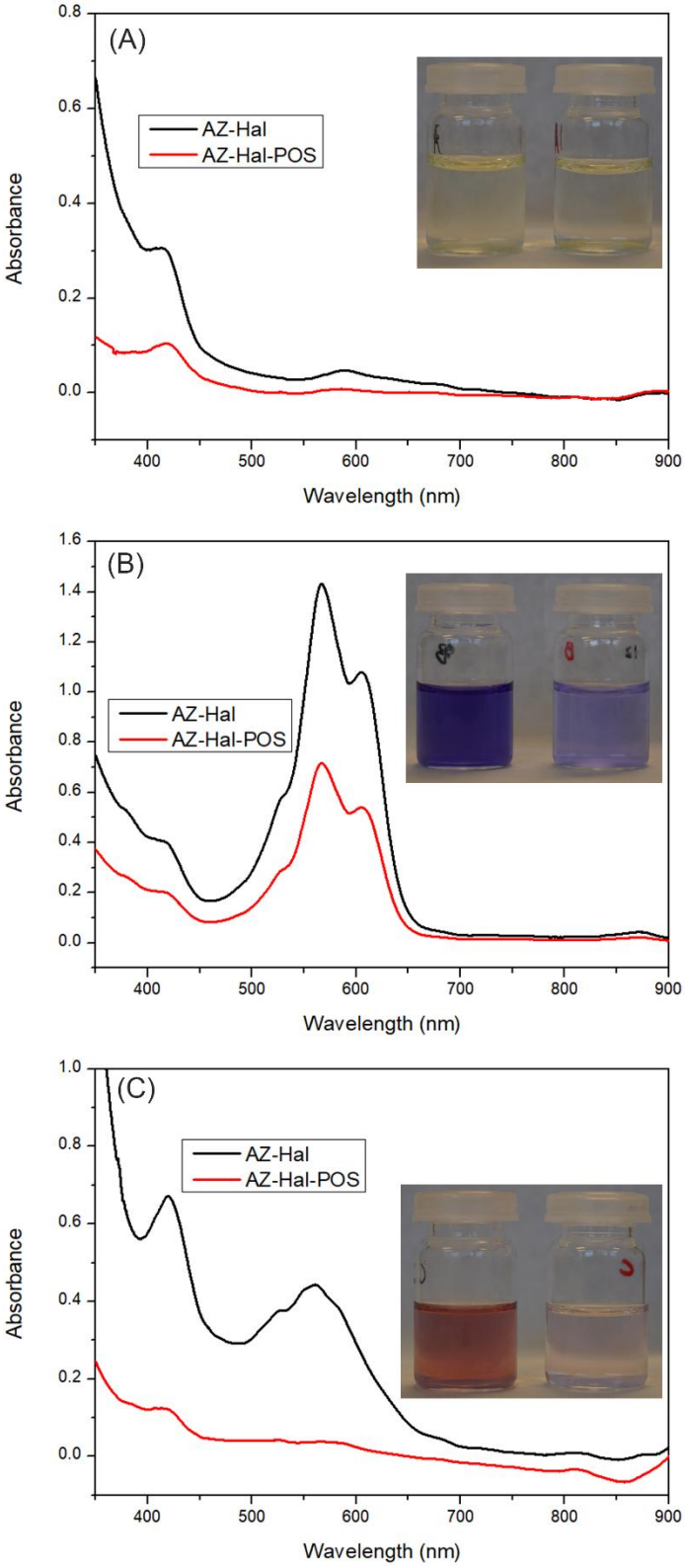

Fig. 9 Absorbance spectra of resulting solution from hybrid pigments treated by (A) 1

mol/L HCl, (B) 1 mol/L NaOH and (C) ethanol.

Covering with POS, the polarity of the surface inverted, from hydrophilicity to hydrophobicity (Fig. 10). When the concentration of organosilane reached at 0.15 mol/L, the contact angle increased to 135°, exhibiting super hydrophobicity. POS is a big crosslinked polymer which tightly packed dye molecules. Thus, aqueous solution and ethanol can not directly contact with dye molecules, resulting in the excellent chemical stability (Fig. 11).

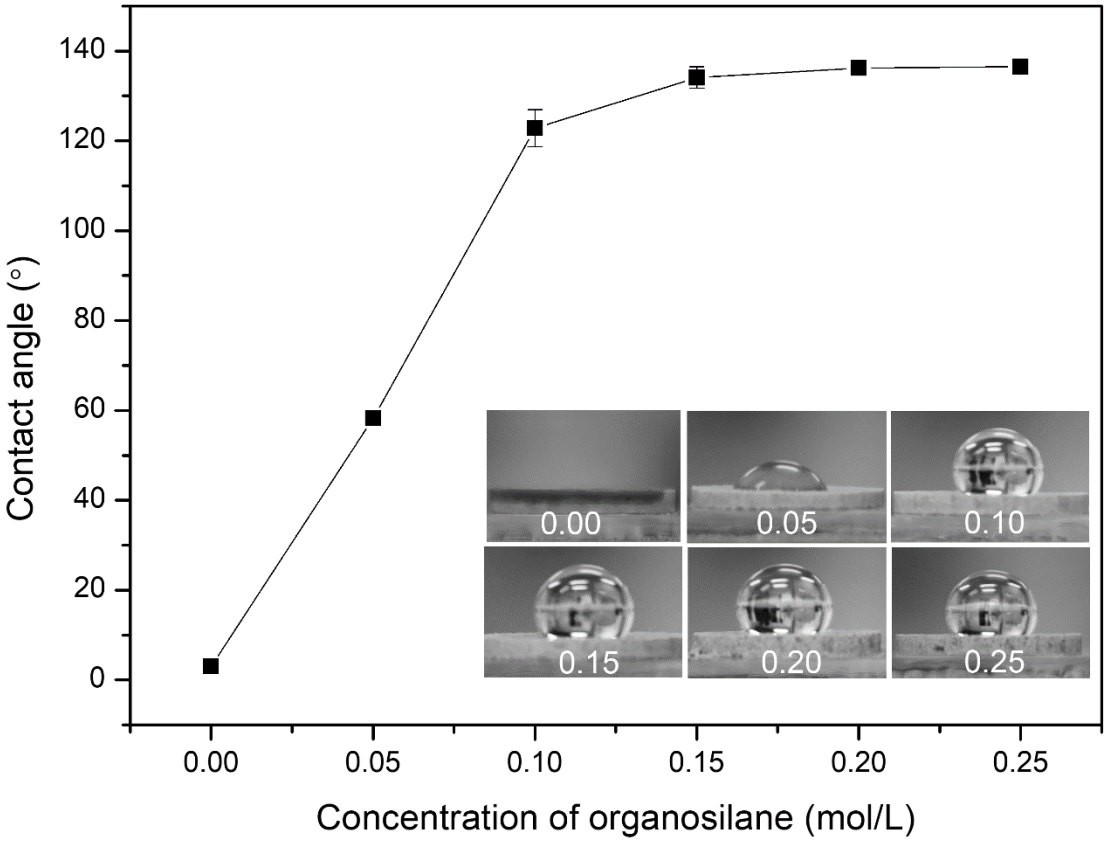

Fig. 10 Contact angle results of AZ-Hal-POS pigment with different concentrations of organosilanes.

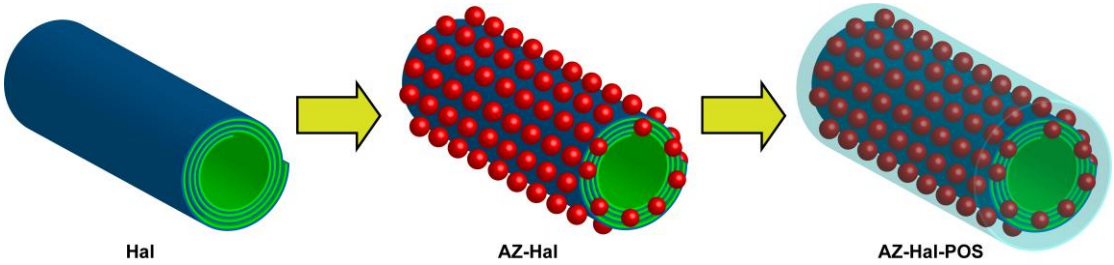

Fig. 11 Interpretive diagram of the chemical stability of AZ-Hal-POS.

Being treated by different chemical solutions not only dissolves the adsorbed dye molecules, but also influences the color of hybrid pigments. The reflectance spectra of treated hybrid pigments (Fig. 12) and the CIE parameters (Table 1 and Table 2) reveal the color changes. The sample names are marked as 'pigment-chemical'. For example, HCl-treated AZ-Hal is labeled as AZ-Hal-HCl. The a* value of AZ-Hal-HCl decreases to 18.7 from 22.8, demonstrating a weaker red color. This is because the dissolution of adsorbed dye molecules. AZ-Hal-NaOH exhibits less red but blue due to the reaction between AZ and OH^-. AZ-Hal-Ethanol presents brighter color because of the dissolution of dye molecules into ethanol. AZ-Hal-POS-NaOH and AZ-Hal-POS-Ethanol show the similar color with AZ-Hal-POS. This fact indicates that the POS layer on the surface protects the dye molecules from reacting with bases and ethanol. However, AZ-Hal-POS-HCl becomes more yellow with the b* value of 21.4, suggesting AZ molecules obtained more protons. Although POS layer prevents dye molecules from dissolving into the solution, H^+ can cross the POS layer and react with dye molecules, resulting in yellow color. As the dye molecules still stay on the Hal surface, the yellow AZ-Hal-POS-HCl can be restored by reacting with basic chemicals. AZ-Hal-POS-HCl was treated with 1 mol/L NaOH for 15 min and the resulting pigment (marked as AZ-Hal-POS-HCl-NaOH) show similar color with

AZ-Hal-POS, with ΔE* of 6.040. The reflectance spectrum of AZ-Hal-POS-HCl-NaOH (Fig. 13) demonstrates the decrease of yellow range.

In a summary, the POS layer not only protects adsorbed dye molecules from dissolving into aqueous solution and organic solvents, but also prevents reacting with chemicals. Although H^+ can cross the POS layer and react with dye molecules, the treated pigments can be restored by neutralization reaction.

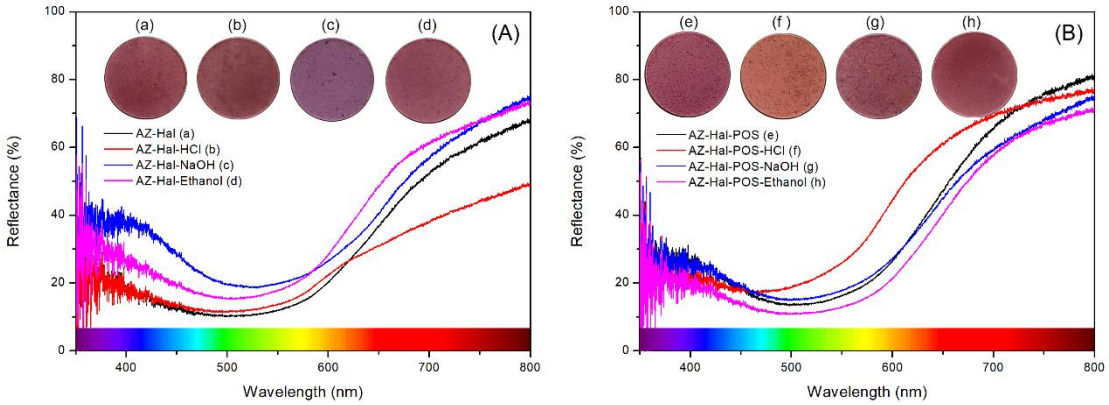

Fig. 12 Reflectance spectra of (A) AZ-Hal and treated with 1mol/L HCl, 1 mon/L NaOH and ethanol for 24 h and (B) AZ-Hal-POS and treated with 1mol/L HCl, 1 mon/L NaOH and ethanol for 24 h.

Table 1 CIE color parameters of AZ-Hal and AZ-Hal treated with different chemicals.

Sample	L*	a*	b*	ΔE*
AZ-Hal	45.9	22.8	6.6	0.0
AZ-Hal-HCl	47.4	18.7	6.8	4.3
AZ-Hal-NaOH	55.3	19.8	-8.1	17.6
AZ-Hal-Ethanol	54.8	23.3	4.7	9.1

Table 2 CIE color parameters of AZ-Hal-POS and AZ-Hal-POS treated with different

chemicals.

Sample	L*	a*	b*	ΔE*
AZ-Hal-POS	50.9	24.8	3.8	0.0
AZ-Hal-POS-HCl	61.4	22.5	21.4	20.8
AZ-Hal-POS-NaOH	52.1	21.2	4.7	3.9
AZ-Hal-POS-Ethanol	48.8	23.8	5.7	3.1
AZ-Hal-POS-HCl-NaOH	56.4	23.0	5.4	6.0

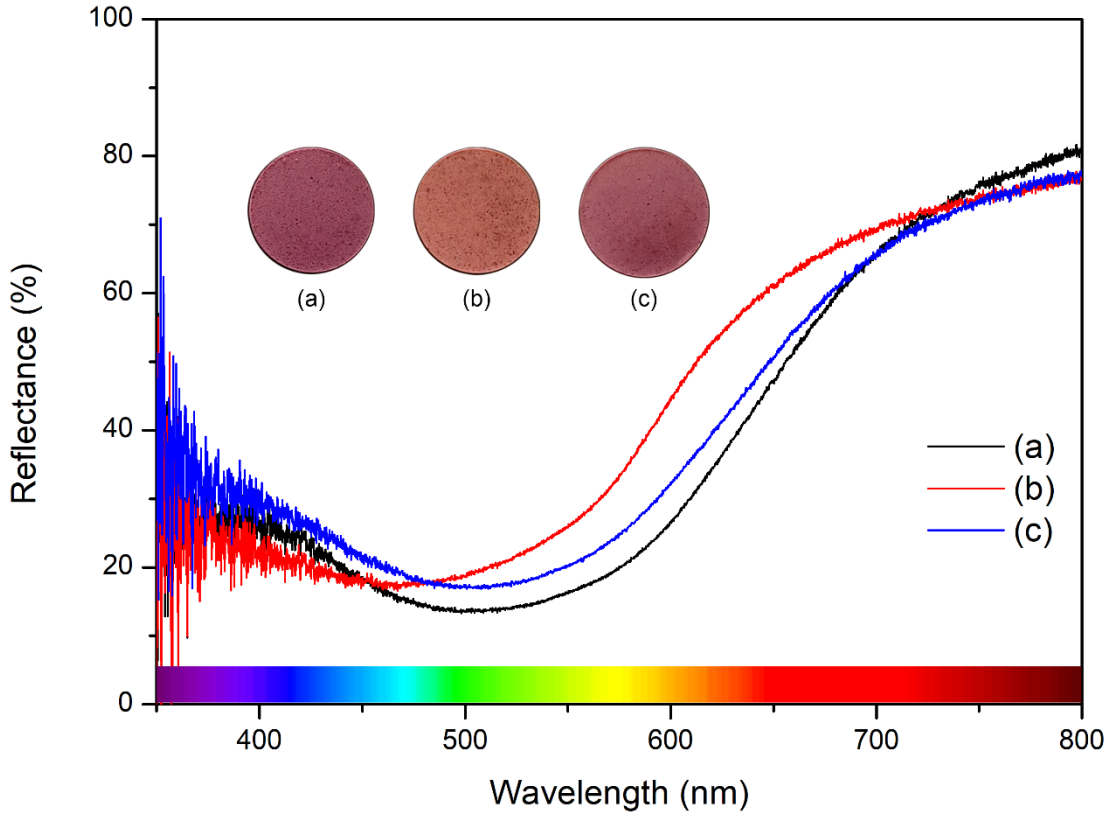

Fig. 13 Reflectance spectra of (a) AZ-Hal-POS, (b) AZ-Hal-POS-HCl and (c) AZ-Hal-POS-HCl-NaOH.

3.3.3 Photostability

Light can be essential for appreciation of artworks, but in long time it may induces deterioration to paintings or other artefacts, causing irreversible damage which may include color fading. Light exposure causes photooxidative degradation resulting in the breakdown of the dye molecules [48]. The colors of hybrid pigments were evaluated before and after light exposure during 360 h, where this time is equivalent to more than 28 years of exposure in a museum.

The spectral reflectance distribution curve of hybrid pigments, before and after photoaging test, are shown in Fig. 14. In general, all samples present similar spectra. The differences are observed for both AZ-Hal and AZ-Hal-POS hybrid pigments where after light exposure,a shift to higher reflection is observed. It is probably due to the degradation/fading of the dye. But we notice that AZ-Hal change more than AZ-Hal-POS, indicating that better resistance of AZ-Hal-POS to light after a long time irradiation. The total color changes presented in Fig. 15 also reveal the color variation of pigment after light exposure by quantitative ΔE* values. AZ-Hal displays higher ΔE* values than AZ-Hal-POS during the light aging process. AZ-Hal shows ΔE* value of 14.3 while AZ-Hal-POS presents the ΔE* value of 10.1 after aging for 360 h. This may be due to the POS layer that prevents dye molecules from contact with oxygen.

According to these results, after light exposure, fading occurs in both hybrid pigments. But hybrid pigment without covering with POS shows more fading than the pigment with POS. AZ-Hal-POS is more stable may be due to the isolation of oxidizing agents (e.g. O_2).

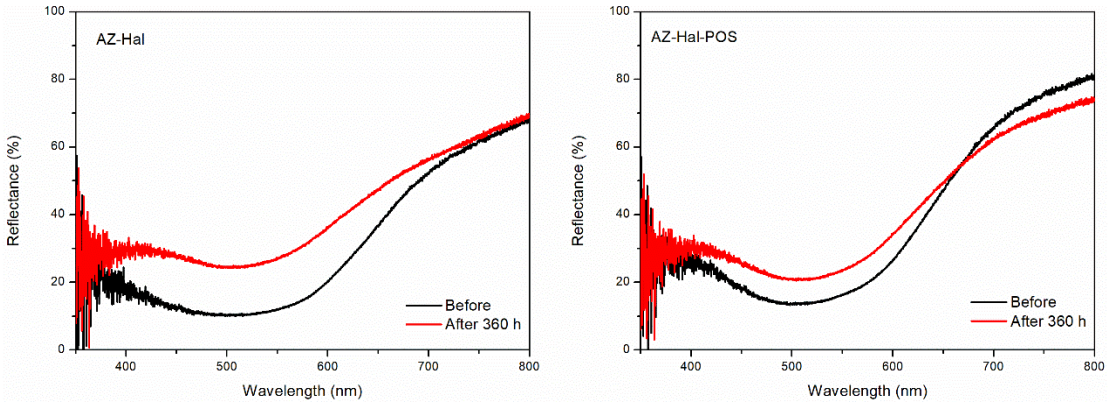

Fig. 14 Reflectance spectra of pigments before and after light exposure for 360 h.

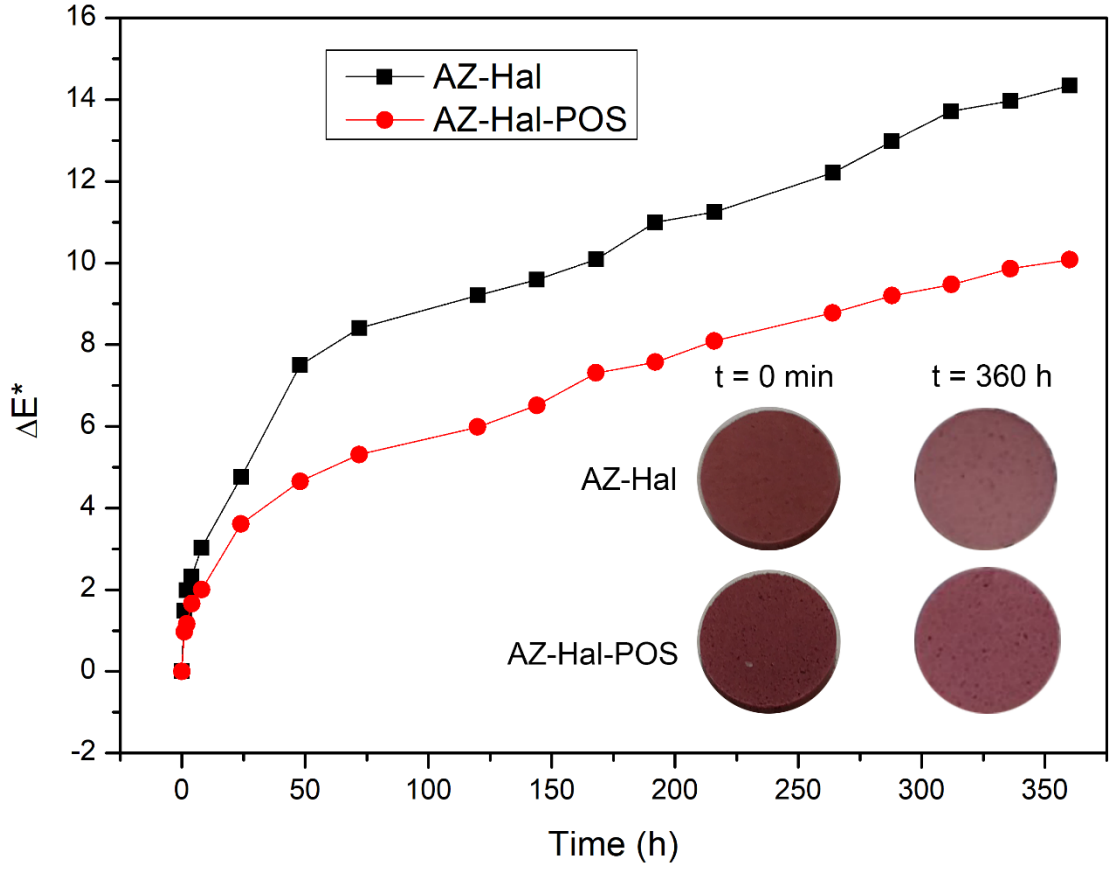

Fig. 15 Color difference of hybrid pigments after light-induced aging for 360 h

4 Conclusion

Hybrid pigments of AZ-Hal were prepared by adsorption in aqueous solution. The adsorption was optimized as pH = 9, concentration of 100 ppm and 1 g of Hal. POS

successfully covered onto the surface of AZ-Hal. XRD and TEM demonstrate that Hal keeps the crystal structure and tubular morphology and AZ (including AZ^- and AZ^{2-}) stays on the surface of the nanotubes. Hydrogen bonds might form between hydroxyl groups of AZ and Hal, as well as the hydroxyl groups with O atoms. AZ-Hal-POS presents super hydrophobicity. Covering with POS didn't obviously change the color of hybrid pigments but enhanced the chemical resistance and photostability by isolating the chemicals such as protons, hydroxides, organic molecules and oxidizing agents. Dye/halloysite hybrid pigments can be a new strategy to enhance the stability of pigments.

Acknowledgment

The support provided by China Scholarship Council (CSC) during the visit of Guanzheng Zhuang (No. 201706400010) to Sorbonne Université is acknowledged.

References

[1] Thompson DV. The materials and techniques of medieval painting: Courier Corporation, 1956.

[2] Saunders D, Kirby J. Light-induced colour changes in red and yellow lake pigments. National Gallery Technical Bulletin. 1994;15(1):79-97.

[3] Tennent N. The deterioration and conservation of dyed historic textiles. Review of Progress in Coloration and Related Topics. 1986;16(1):39-45.

[4] Taylor G. Natural dyes in textile applications. Review of Progress in Coloration

and related topics. 1986;16(1):53-61.

[5] Claro A, Melo MJ, Schäfer S, de Melo JSS, Pina F, van den Berg KJ, et al. The use of microspectrofluorimetry for the characterization of lake pigments. Talanta. 2008;74(4):922-9.

[6] Palit DK, Pal H, Mukherjee T, Mittal JP. Photodynamics of the S1 state of some hydroxy-and amino-substituted naphthoquinones and anthraquinones. Journal of the Chemical Society, Faraday Transactions. 1990;86(23):3861-9.

[7] Bechtold T, Mussak R. Handbook of natural colorants: John Wiley & Sons, 2009.

[8] de Viguerie L, Jaber M, Pasco H, Lalevée J, Morlet- Savary F, Ducouret G, et al. A 19th Century "Ideal" Oil Paint Medium: A Complex Hybrid Organic–Inorganic Gel. Angewandte Chemie International Edition. 2017;56(6):1619-23.

[9] Miliani C, Romani A, Favaro G. Acidichromic effects in 1, 2-di-and 1, 2, 4-trihydroxyanthraquinones. A spectrophotometric and fluorimetric study. Journal of Physical Organic Chemistry. 2000;13(3):141-50.

[10] Pérez E, Ibarra IA, Guzmán A, Lima E. Hybrid pigments resulting from several guest dyes onto γ-alumina host: A spectroscopic analysis. Spectrochimica Acta Part A: Molecular and Biomolecular Spectroscopy. 2017;172:174-81.

[11] Río MSD, Doménech A, Doménech-Carbó MT, Suárez M, García-Romero E. Chapter 18 - The Maya Blue Pigment. Development in Clay Science: Elsevier Ltd; 2011. p. 453-81.

[12] Fournier F, Viguerie LD, Balme S, Janot JM, Walter P, Jaber M. Physico-chemical characterization of lake pigments based on montmorillonite and

carminic acid. Appl Clay Sci. 2016;130:12-7.

[13] Mahmoodi A, Ebrahimi M, Khosravi A, Mohammadloo HE. A hybrid dye-clay nano-pigment: Synthesis, characterization and application in organic coatings. Dyes & Pigments. 2017;115(4):811-5.

[14] Raha S, Quazi N, Ivanov I, Bhattacharya S. Dye/Clay intercalated nanopigments using commercially available non-ionic dye. Dyes and Pigments. 2012;93(1–3):1512-8.

[15] Trigueiro P, Rodrigues F, Rigaud B, Balme S, Janot J-M, dos Santos IM, et al. When anthraquinone dyes meet pillared montmorillonite: Stability or fading upon exposure to light? Dyes and Pigments. 2018;159:384-94.

[16] Epstein M, Yariv S. Visible-spectroscopy study of the adsorption of alizarinate by Al-montmorillonite in aqueous suspensions and in solid state. J Colloid Interf Sci. 2003;263(2):377-85.

[17] Guillermin D, Debroise T, Trigueiro P, de Viguerie L, Rigaud B, Morlet-Savary F, et al. New pigments based on carminic acid and smectites: A molecular investigation. Dyes and Pigments. 2018;160:971-82.

[18] Brito DF, da Silva Filho EC, Fonseca MG, Jaber M. Organophilic bentonites obtained by microwave heating as adsorbents for anionic dyes. Journal of environmental chemical engineering. 2018;6(6):7080-90.

[19] Pereira FA, Sousa KS, Cavalcanti GR, França DB, Queiroga LN, Santos IM, et al. Green biosorbents based on chitosan-montmorillonite beads for anionic dye removal. Journal of Environmental Chemical Engineering. 2017;5(4):3309-18.

[20] Tangaraj V, Janot J-M, Jaber M, Bechelany M, Balme S. Adsorption and photophysical properties of fluorescent dyes over montmorillonite and saponite modified by surfactant. Chemosphere. 2017;184:1355-61.

[21] Dong J, Wang Q, Zhang Y, Zhu Z, Xu X, Zhang J, et al. Colorful Superamphiphobic Coatings with Low Sliding Angles and High Durability Based on Natural Nanorods. Acs Appl Mater Inter. 2016;9(2):1941.

[22] Fan L, Zhang Y, Zhang J, Wang A. Facile preparation of stable palygorskite/cationic red X-GRL@ SiO 2 “Maya Red” pigments. RSC ADVANCES. 2014;4(108):63485-93.

[23] Giustetto R, Seenivasan K, Pellerej D, Ricchiardi G, Bordiga S. Spectroscopic characterization and photo/thermal resistance of a hybrid palygorskite/methyl red Mayan pigment. Microporous & Mesoporous Materials. 2012;155(11):167-76.

[24] Zhang Y, Fan L, Chen H, Zhang J, Zhang Y, Wang A. Learning from ancient Maya: Preparation of stable palygorskite/methylene blue@SiO 2 Maya Blue-like pigment. Microporous & Mesoporous Materials. 2015;211:124-33.

[25] Zhang Y, Zhang J, Wang A. Facile preparation of stable palygorskite/methyl violet@SiO2 "Maya Violet" pigment. Journal of Colloid & Interface Science. 2015;457:254.

[26] Zhang Y, Zhang J, Wang A. From Maya blue to biomimetic pigments: durable biomimetic pigments with self-cleaning property. Journal of Materials Chemistry A. 2016;4(3):901-7.

[27] Giustetto Kalvachev Y, Jaber M, Mavrodinova V, Dimitrov L, Valtchev V, Seeds-induced fluoride media synthesis of nanosized zeolite Beta crystals, Microporous & Mesoporous Materials, 2013;177:129-141.

[28] Giustetto R, Wahyudi O, Corazzari I, Turci F. Chemical stability and dehydration behavior of a sepiolite/indigo Maya Blue pigment. Appl Clay Sci. 2011;52(1-2):41-50.

[29] Ovarlez S, Chaze A-M, Giulieri F, Delamare F. Indigo chemisorption in sepiolite. Application to Maya blue formation. Comptes Rendus Chimie. 2006;9(10):1243-8.

[30] Ovarlez S, Giulieri F, Chaze AM, Delamare F, Raya J, Hirschinger J. The Incorporation of Indigo Molecules in Sepiolite Tunnels. Chemistry - A European Journal. 2009;15(42):11326-32.

[31] Ovarlez S, Giulieri F, Delamare F, Sbirrazzuoli N, Chaze AM. Indigo-sepiolite nanohybrids: Temperature-dependent synthesis of two complexes and comparison with indigo-palygorskite systems. Microporous & Mesoporous Materials. 2011;142(1):371-80.

[32] Rondão R, Seixas de Melo JSr. Thio-Mayan-like Compounds: Excited state characterization of indigo sulfur derivatives in solution and incorporated in palygorskite and sepiolite clays. The Journal of Physical Chemistry C. 2012;117(1):603-14.

[33] Tian G, Wang W, Mu B, Wang Q, Wang A. Cost-efficient, vivid and stable red hybrid pigments derived from naturally available sepiolite and halloysite. Ceramics International. 2017;43(2):1862-9.

[34] Joussein E. Chapter 2 – Geology and Mineralogy of Nanosized Tubular Halloysite. Developments in Clay Science2016. p. 12-48.

[35] Bate TF. Morphology and structure of endellite and halloysite. American Mineralogist. 1950;35.

[36] Churchman, Davy GJ, Aylmore TJ, Gilkes LAG, Self RJ, P. G. Characteristics of Fine Pores in Some Halloysites. Clay Miner. 1995;30(2):89-98.

[37] Zhang A, Mu B, Luo Z, Wang A. Bright blue halloysite/CoAl 2 O 4 hybrid pigments: Preparation, characterization and application in water-based painting. Dyes & Pigments. 2017;139:473-81.

[38] Micó- Vicent B, Martínez- Verdú FM, Novikov A, Stavitskaya A, Vinokurov V, Rozhina E, et al. Stabilized dye–pigment formulations with platy and tubular nanoclays. Advanced Functional Materials. 2017:1703553.

[39] Kuban V, Havel J. Some 2-(2-thiazolylazo)-4-methoxyphenol (TAMP) complex equilibria. 1. Acid -base properties of tamp in water and in various mixed solvents. . Acta Chemica Scandinavica. 1973;27(2):528-40.

[40] Pasbakhsh P, Churchman GJ, Keeling JL. Characterisation of properties of various halloysites relevant to their use as nanotubes and microfibre fillers. Appl Clay Sci. 2013;74:47-57.

[41] Canamares M, Garcia- Ramos J, Domingo C, Sanchez- Cortes S. Surface- enhanced Raman scattering study of the adsorption of the anthraquinone pigment alizarin on Ag nanoparticles. Journal of Raman Spectroscopy. 2004;35(11):921-7.

[42] Koperska M, Łojewski T, Łojewska J. Vibrational spectroscopy to study degradation of natural dyes. Assessment of oxygen-free cassette for safe exposition of artefacts. Analytical and bioanalytical chemistry. 2011;399(9):3271-83.

[43] Socrates G. Infrared and Raman characteristic group frequencies: tables and charts: John Wiley & Sons, 2001.

[44] Cheng H, Frost RL, Yang J, Liu Q, He J. Infrared and infrared emission spectroscopic study of typical Chinese kaolinite and halloysite. Spectrochimica Acta Part A: Molecular and Biomolecular Spectroscopy. 2010;77(5):1014-20.

[45] Cheng H, Yang J, Liu Q, Zhang J, Frost RL. A spectroscopic comparison of selected Chinese kaolinite, coal bearing kaolinite and halloysite—A mid-infrared and near-infrared study. Spectrochimica Acta Part A: Molecular and Biomolecular Spectroscopy. 2010;77(4):856-61.

[46] Poch O, Jaber M, Stalport F, Nowak S, Georgelin Th, Lambert J-F, Szopa C, and Coll P, Effect of Nontronite Smectite Clay on the Chemical Evolution of Several Organic Molecules under Simulated Martian Surface Ultraviolet Radiation Conditions, Astrobiology, 2015, 15(3), 221-237.

[47] Yuan P, Southon PD, Liu Z, Green ME, Hook JM, Antill SJ, et al. Functionalization of halloysite clay nanotubes by grafting with γ-aminopropyltriethoxysilane. The Journal of Physical Chemistry C. 2008;112(40):15742-51.

[48] Feng W, Nansheng D, Helin H. Degradation mechanism of azo dye CI reactive red 2 by iron powder reduction and photooxidation in aqueous solutions.

Chemosphere. 2000;41(8):1233-8.